Vacuum 137 (2017) 155–162

Contents lists available at ScienceDirect

Vacuum

journal homepage: www.elsevier.com/locate/vacuum

Surface structure and electric properties of nitrogen incorporated NCD films

Qi Sun [a], Jianhua Wang [a, b, *], Jun Weng [a], Fan Liu [a]

[a] Key Laboratory of Plasma Chemistry and Advanced Materials of Hubei Province, Wuhan Institute of Technology, Wuhan 430070, PR China
[b] Institute of Plasma Physics, Chinese Academy of Science, Hefei 230031, PR China

ARTICLE INFO

Article history:
Received 22 August 2016
Received in revised form
22 December 2016
Accepted 23 December 2016
Available online 27 December 2016

Keywords:
Nitrogen rich plasma
N incorporated
Electric performance
NCD

ABSTRACT

Linear characteristics were shown in I-V curves for nanocrytalline diamond (NCD) films deposited in a nitrogen rich atmosphere by microwave plasma chemical vapor deposition (MPCVD). In order to figure out how grain size, fraction and structure of N incorporated NCD films influence the electric performances of NCD films, the scanning electron microscopy (SEM), X-ray diffractometer (XRD), X-ray photoelectron spectroscopy (XPS) and Raman spectroscopy were applied. Different surface morphologies are shown while the nitrogen concentration was varied. A similar tendency of electrical conductivity change versus grain size decrease and grain boundary network increase in NCD films has been observed. C1s core-energy, N1s core-energy and Raman spectra showed that the fraction and the chemical bonds of carbon atoms varied when the N_2 concentration in plasma was different. All these measurements indicate that N_2 concentration in plasma is a critical parameter for the growth, grain size, chemical bond and the electrical performance of deposited NCD films.

1. Introduction

Diamond film synthesis can be traced back to 1950s [1], while most of studies had focused on the production of microcrystalline diamond film due to its extremely outstanding properties [2,3]. Performance of microcrystalline diamond films cannot satisfy the increasingly stringent demands in small device areas. Without changing structure or composition of diamond, the optimized diamond properties can only be achieved by changing its microstructure [4]. Diamond films with grain size of tens to hundreds of nanometers (mainly from 10 to 100 nm) are classified as nanocrystalline diamond (NCD) films [5]. It is generally believed that hydrogen plays an important role in the processes of various diamond depositions [6]. It was found that diamond crystalline sizes and morphologies were controllable by adding noble gas into growth plasma. Both pure argon/CH_4 [7] and hydrogen-poor/Ar-rich/CH_4 gas mixtures [8] plasma can be applied to deposit NCD films. D. Zhou et al. [9] had systematically studied the behavior of diamond films deposited with various concentration of argon, from 2% to 98%. E.M.A. Fuentes-Fernandez et al. [10] had systemically studied the growth of MCD to NCD to UNCD films by using the hot filament chemical vapor deposition technique. O. Auciello and A.V. Sumant had carefully disused the science, technology and application of nitrogen doped NCD and UNCD films [8]. In order to investigate the electrical conductivity of nitrogen incorporated nanocystalline diamond films, J. Birrell et al. [11], T.D. Corrigan et al. [12] and Qingyun Chen et al. [13] replaced hydrogen with nitrogen in the argon plasma. As reactive gas nitrogen is more advantageous and it has been proved that proper addition of nitrogen in plasma is helpful to decrease the diamond grains and benefit the deposited NCD films in a conventional CH_4/H_2 deposition system [14]. N incorporated NCD films are obtained mainly by two approaches. The first approach is N ion implantation after deposition of NCD films which are commonly used to modify the film surface like inducting defects or amorphous carbon in the films [15]. The second one is to introduce nitric gas into the chamber during the process which can achieve nitrogen atom doping without damaging the surface structure [16]. So the microwave plasma CVD method was chosen to deposit NCD films in this study.

NCD films have many special properties which make them well candidates for many applications [8]. For example, the smooth surface and low coefficient of friction make them possible to be

* Corresponding author. Key Laboratory of Plasma Chemistry and Advanced Materials of Hubei Province, Wuhan Institute of Technology, Wuhan 430070, PR China, Tel.: +86 17771495139; fax: +86 027 87194533.
E-mail addresses: anitasun2015@163.com (Q. Sun), WangJianhuaWIT@163.com (J. Wang), 951152515@qq.com (J. Weng), 84312739@qq.com (F. Liu).

http://dx.doi.org/10.1016/j.vacuum.2016.12.040
0042-207X/

used in the protecting, wear and sealing coating field [17,18]. The excellent mechanical properties and chemical inertness make them been wildly used on MEMS/NEMS devices [19,20]. Meanwhile, special conductivity accompanied with outstanding biocompatibility enables NCD films to be considered as the best candidates of electrochemically sensitive and stable electrodes [21]. The doping of nitrogen atom into the NCD films improves the electric performances [22]. The content of doped nitrogen atoms are always considered as the main factor which affected the conductivity of NCD films [23,24], but the studies of Kalpataru Panda et al. [16], and T.D. Corrigan et al. [12] showed that the varying of the volume of the grain boundaries and the structure of grain boundaries were the main reasons which lead to the change of the conductivity of the nitrogen incorporated nanocrystalline diamond films. The doping of nitrogen atoms mainly happened at grain boundaries [25,26] and affected the conductivity by promoting sp^2 bonding in the neighboring carbon atoms [12].

Comparing to conventional percentage of nitrogen gas in plasma [13,27], this work applied a rich nitrogen atmosphere to deposit N incorporated NCD films. The volume of grain boundaries and chemical bonded type of the sp^2 carbon are considered as the main factors which affect the films' electric performance. Various methods were taken to characterize the deposited samples.

2. Experimental details

A 2 kW Alter SM840E 2.45 GHz MPCVD device was used with a N_2-rich $CH_4/H_2/N_2$ gas system. Silicon wafers with 1 × 1 cm^2 and 0.5 mm in thickness were mechanically pre-scratched with 0.5 μm diamond powder for 15 min to enhance diamond nucleation. Then, the substrates were ultrasonically cleaned with acetone, deionized water for 5 min respectively and inserted into the reactor chamber after being dried in nitrogen flow. A molybdenum plate, 100 mm in diameter and 5 mm in thickness, was used as the substrate holder.

Before the deposition of diamond films, the reactor chamber was cleaned by the hydrogen plasma which was induced with a microwave power of 1.0 kW at a total pressure of 28 torr while hydrogen flow rate was 200 sccm. The deposition process consisted of two steps: nucleation and growth. Same nucleation parameters were set for all samples, which is 1.2 kW for microwave power, 30 torr for gas pressure, and 750 °C for the nucleation temperature. A thermal couple under the substrate holder was used to monitor the temperature of the substrate. In the growth step, nitrogen was introduced into the reactor chamber and the deposition parameters were listed in Table 1. In order to investigate the effects of rich N_2 incorporation on the microstructure, grain size and quality of diamond films, the N_2 concentration in $CH_4/H_2/N_2$ gas system was varied in a range from 70% to 95% in the total gas flow rate.

To observe the electric behavior of the NCD films with different N_2 concentrations, the I-V measurements were performed by using the PARSTAT 4000 Analyzer produced by Princeton Applied Research. The surface morphologies and microstructures of the samples were characterized by scanning electron microscopy (JSM 5510LV, operated at 128 keV electron energy and high resolution). FALCON type X-ray powder diffractometer (X-ray source for Cu Kα X-radiation, the wavelength of 1.5418 Å, EDAX) was used to measure the phase composition and grain size of the films. X-ray photoelectron spectroscopy (ESCALAB, 250Xi) and Raman

Table 1
Parameters and grain size of the deposited NCD films.

No.	Grains size/nm	N_2/sccm	H_2/sccm	CH_4/sccm	Pressure/torr	Microwave power/kW	Substrate temperature/°C
S1	25	70	20	10			
S2	17	80	10	10			
S3	10	85	5	10	35	1.5	980
S4	15	90	0	10			
S5	20	95	0	5			

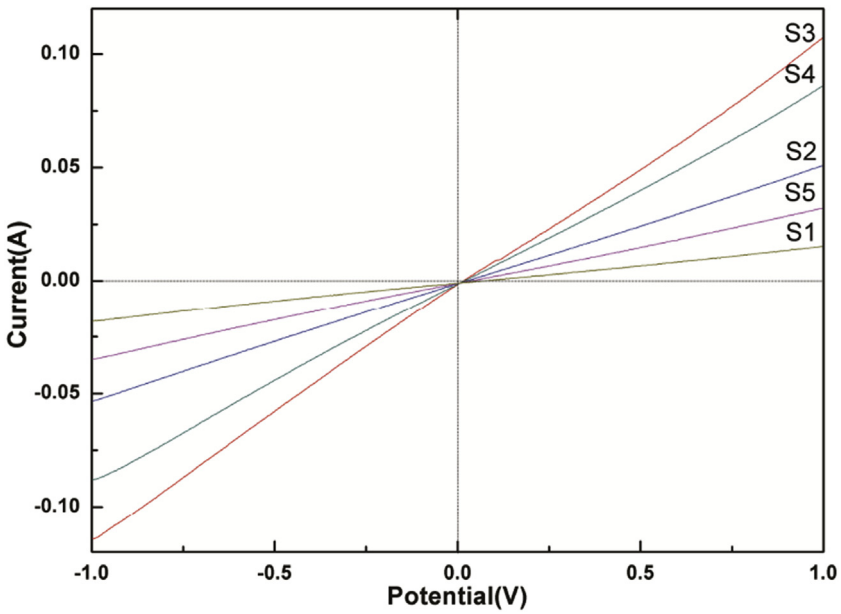

Fig. 1. I–V curves of NCD films deposited with different nitrogen concentrations.

spectrometer (Renishaw, RM1000) to investigate the surface bonding states of deposited samples.

3. Results and discussion

Fig. 1 provides the I-V curves of samples deposited with varying nitrogen concentrations (from 70% to 95%) and all samples present a linear (Ohmic) characteristic which suggests that in a nitrogen rich and hydrogen poor atmosphere conductive NCD films can be obtained. S1 to S5 in Fig. 1 are samples which is list in Table 1. As it is shown in Fig. 1 the continuously increasing nitrogen concentrations are not companied with a keeping increasing conductivity of deposited films. When the nitrogen increased from 70% to 85% the conductivity kept increasing however a rectification phenomenon appears at 90% of nitrogen in plasma. Similar phenomenon was observed with low nitrogen concentration in the $CH_4/Ar/N_2$ atmosphere [28], but the phenomenon of the appearance of minimum value in N_2-rich is more obvious than it in the low concentration of nitrogen atmosphere.

The surface morphologies of all deposited samples are shown in Fig. 2. From Fig. 2(a)–2(e) are surface SEM images of samples deposited with different nitrogen concentrations. All films consisted of nanosized grains which are similar to the diamond films with an Ar-rich $H_2/CH_4/N_2$ ambient [29,30]. In Fig. 2(a), with 70% of the N_2, the surface morphology shows faceted diamond microstructures with granular grains and is obviously coarser than films deposited with other N_2 concentrations. When increased the N_2 concentration to 80%, the "needle-like" diamond grains appear, but the film surface is still dominated by granular grains. Further increased the N_2 concentration to 85%, granular grains disappear while film surface is covered by needle-like grains. With even higher concentration of N_2 (90%), the needle-like grains is disappearing. The surface morphology finally turned out to the cauliflower like when the N_2 concentration is 95%. Fig. 2(f) is the cross-section SEM image of S3 and the inset of Fig. 2 (f) is a cross-section SEM image of a MCD film deposited in our laboratory. Apart from the typical columnar growth of microcrystal diamond as the inset of Fig. 2(f) showed diamond films deposited in this study appear as an obvious nanographite films with lamellae structure [8,12,31]. After 12 h of deposition the thickness of sample 3 was

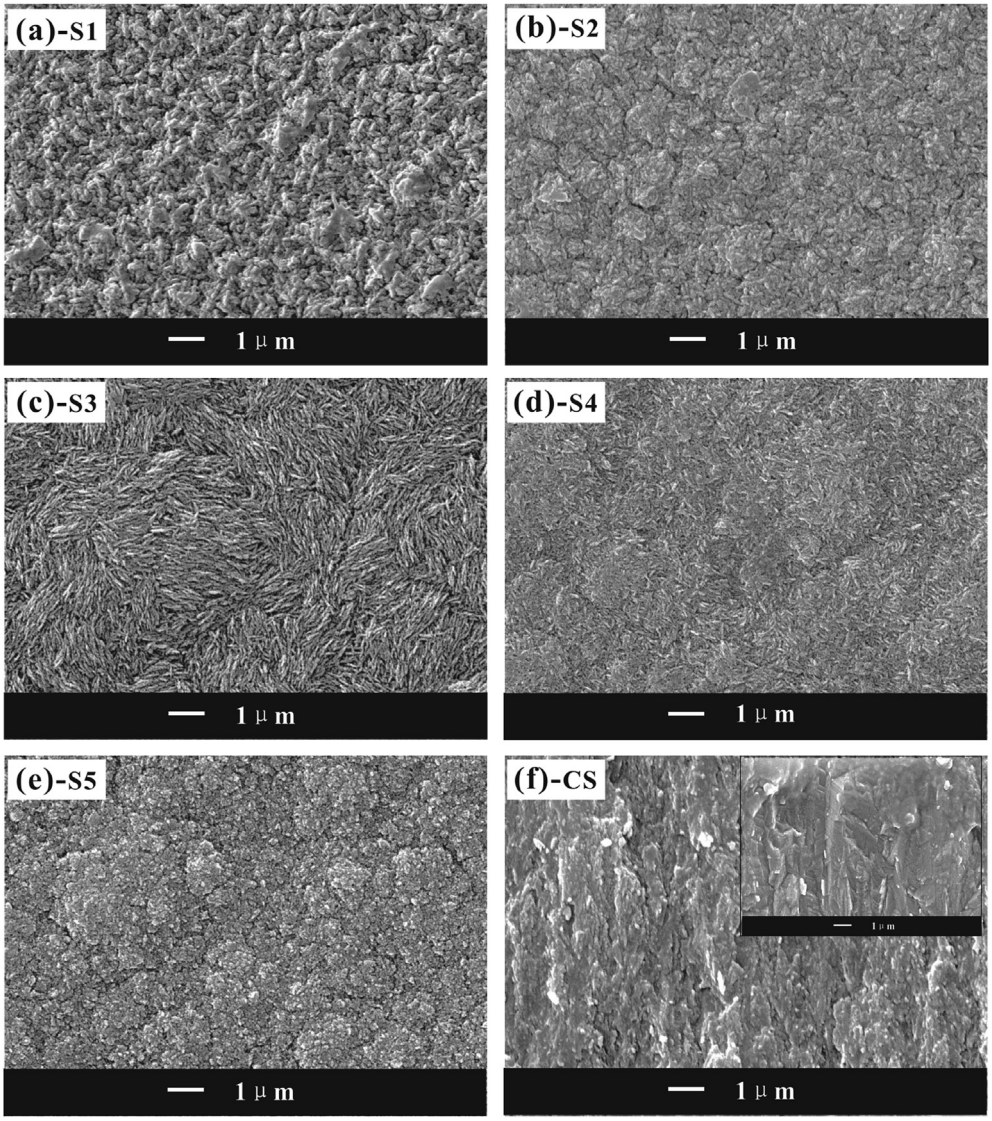

Fig. 2. SEM images of NCD films deposited with different nitrogen concentrations: (a)-S1, (b)-S2, (c)-S3, (d)-S4, (e)-S5, (f)-cross section of S3, the inset of (f)-cross section of MCD deposited in our lab.

28.6 μm, and the average growth of NCD films was 2.38 μm/h.

From the SEM results it can be concluded that NCD films can be obtained in a N_2-rich N_2-CH_4-H_2 mixture atmosphere and the varying concentration of N_2 can significantly affect the surface morphologies of deposited NCD films. The grain form switches from granular type to needle-like one and finally present like cauliflowers. Other parameters were kept constant while N_2 concentration in plasma was the only changing parameter as it was shown in Table 1, so it can be deduced that N_2 in the gas mixture can significantly affect the growth and surface morphologies of deposited NCD films.

In order to better understand the growth and the relationship between the surface morphology and grain size of deposited NCD films with different N_2 concentrations the X-ray diffraction (XRD) was used. The XRD patterns of all deposited samples films are shown in Fig. 3. The relatively sharp and narrow diffraction peaks at 43.9 °, 75.5 °and 91.8 ° are identified to be diamond (111), (220) and (311) diffraction peaks, respectively. Peak (111) appears in all XRD patterns of deposited samples and the intensity increases with the increasing of nitrogen concentration from 70% to 85% and decreases when the nitrogen concentration changes from 90% to 95%. Peak (220) is almost invisible for the concentration of 70% and 80% and the intensity increases with the increasing of the nitrogen concentration accompanied with a broadness of peaks. While for peak (311), it is apparent in all samples except for the concentration of 70% and the intensity is also increasing with the addition of nitrogen concentrations.

The transition of XRD patterns not only suggests a transform of the growth pattern but also indicates the change of grain size. The well-known Sherrer equation [32] was applied to calculate the grain sizes of the NCD films deposited at different nitrogen concentrations:

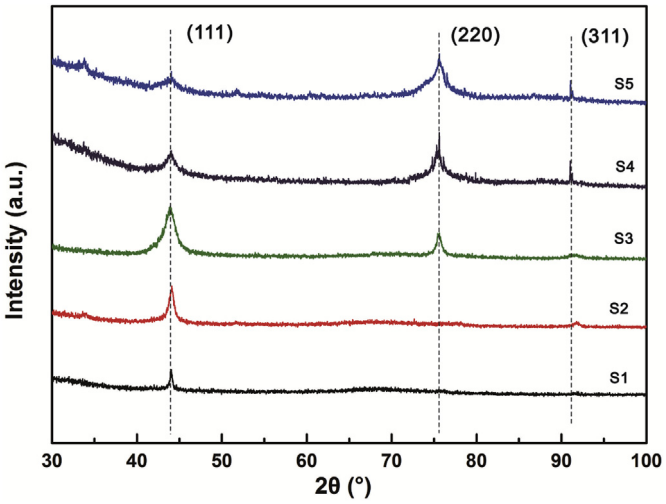

Fig. 3. XRD patterns of NCD films deposited with different N_2 concentrations.

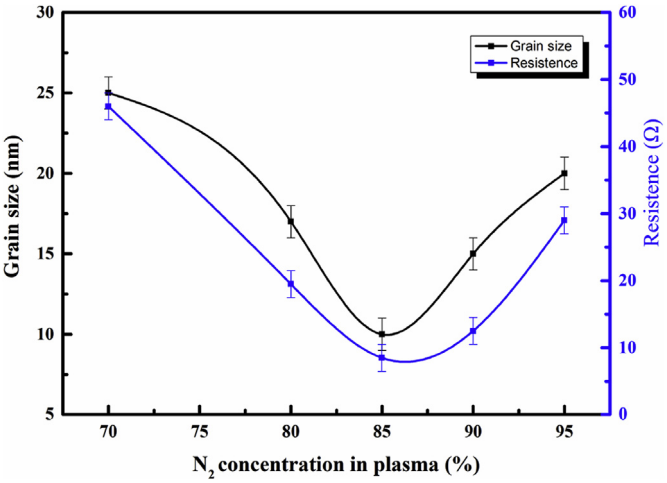

Fig. 4. Grain size and resistance of deposited films with different nitrogen concentrations and the vertical bars represent the value of value variation of grain sizes and resistances.

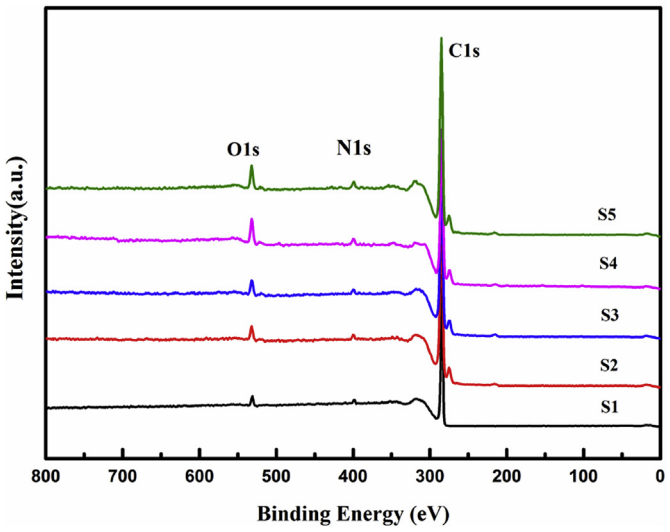

Fig. 5. X-ray photoemission spectra of NCD films deposited with different nitrogen concentrations.

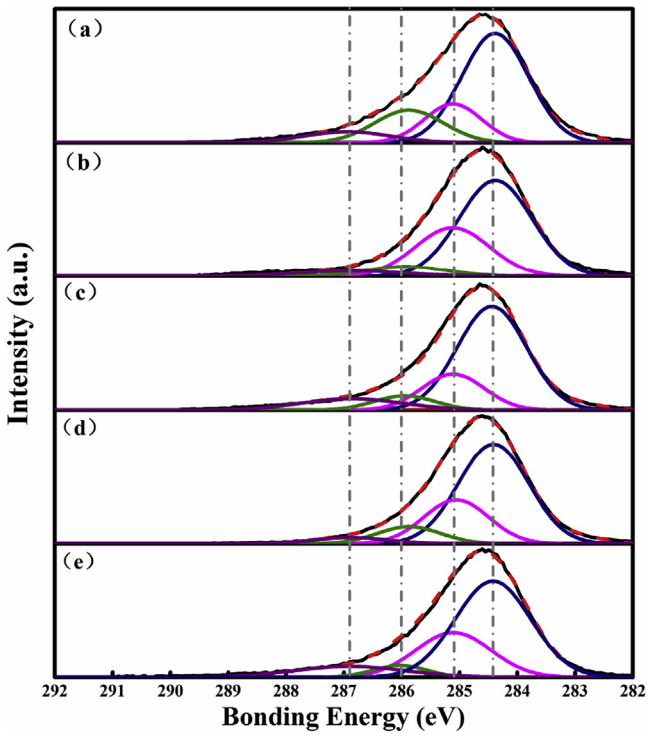

Fig. 6. C1s core-energy level spectra for NCD films deposited with different nitrogen concentrations (a)-S1, (b)-S2, (c)-S3, (d)-S4, (e)-S5.

$$d = 0.9\,\lambda/B\cos\theta$$

Here *d* is the grain size, $\lambda = 1.54016$ Å and *B* is the full width at half maximum (FWHM) of the diamond diffraction peak. The grain sizes are obtained from diamond (111) X-ray diffraction peak, and the calculating results are list in Table 1. It is obvious that the variation of the N_2 concentration can significantly affect the grain size of the diamond films. When the nitrogen concentration increase from 70% to 85% the grain sizes decrease from 25 nm to 10 nm. While the concentration keeps increasing the grain size increase and reaches 20 nm when the concentration is 95% for nitrogen in plasma. This tendency is same to the previous observation as SEM images. For better analysis and comparison, the values of grain sizes and resistances of all NCD films are shown in Fig. 4. It shows that resistance is decreasing while the grain size is decreasing and the increasing grain size is accompanied with the increasing of the resistance. The decrease of grain size leaded to the increase of the amount of the grain boundaries, this was also proved by the study of Chii-Ruey Lin et al. [31]. The study of them also showed that the smaller grain size was accompanied with the broadened of the width of the grain boundaries. Meanwhile, the study of James Birrell et al. [25] showed that the doping of nitrogen can only slightly increase the amount of the sp^2 carbon in deposited samples and the grain itself remained purified diamond while the overall grain boundary of N-doped nano-grains diamond films. So we can deduce that the obviously changing of the surface morphologies were caused by the changing of the grain sizes of deposited NCD samples with different N_2 concentration in plasma.

For better understanding of the conductivity mechanism of nitrogen-doped NCD films, the X-ray photoemission spectroscopy (XPS) was applied to investigate the surface chemistry of deposited films. The complex surface structure and the relationship of the conductivity of deposited films will be discussed. In Fig. 5 the survey XPS spectra of NCD films deposited with different nitrogen concentrations are presented. An apparent peak around 400 eV is shown for all samples, which corresponds to the nitrogen atoms in carbon film lattice [33]. The peak intensity keeps increasing while the nitrogen concentration increases from 70% to 95%. A strong C1s peak is shown at 285.0 eV [33]. The existence of oxygen may due to the exposure in the air during the waiting period before XPS examination.

To better analysis the composition of deposited films with different nitrogen concentration, the C1s core-energy level spectra of all samples were collected and are shown in Fig. 6. All C1s spectra were decomposed into four components: 284.4 eV, the sp^2 hybridized carbon known as C=C [34]; 285.1 eV, the sp^3 bulk carbon known as C-C [34–36]; 286.0 eV for C=N bonds and 286.9 eV for C-N bonds [34]. The deconvolution result shows that the varying concentration of nitrogen not only affected the grain size of the deposited films but also influenced the chemical bonds of the carbon atoms of deposited films. As it is shown in Fig. 7, the fraction of sp^2 bonded carbon reaches the maximum when the nitrogen concentration is 85% and the varying sp^2 fraction has a similarity to the changing tendency of the grain size and the resistance of NCD films which is presented in Fig. 4. According to the study of James Birrell et al. the diamond grains remain pure diamond after nitrogen is added to the film [25], so the increasing of sp^2 bond carbon content is main happened at the grain boundaries. According to the deconvolution result the nitrogen concentration can significantly affect the chemical bonds of the deposited films which finally affected the conductivity in macroscopic. The sp^2 structure is always considered as the defects in grain boundaries [37], which can apply the conductive channel for electrons. So it can be deduced that the smaller the grain size is, the larger the sp^2 amount is. Increasing of the surface conductivity is accordant to the decreasing of grain size, which reaches the minimum at 85% of nitrogen in plasma.

The Raman spectroscopy was applied to further measure the structure of deposited films, because the Raman scattering is very sensitive to the π-bonded sp^2 carbon [7]. The wavelength of the used laser was 633 nm. Fig. 8 presents the Raman spectra of NCD films deposited with 70%–95% N_2 in the $N_2/H_2/CH_4$ atmosphere and Gussian fitting was applied to fit the Raman spectra. Some common peaks of NCD films are shown: (1) peaks around 1350 cm^{-1} (D-band) is the signature of sp^2 bonded carbon which existed in rings only, (2) the 1580 cm^{-1} peak of graphite G band arising from the in-plane stretching mode of sp^2-bond carbon at grain boundaries which existed in chains and rings both, (3) peaks around 1150 cm^{-1} and 1480 cm^{-1} are related to the trans-

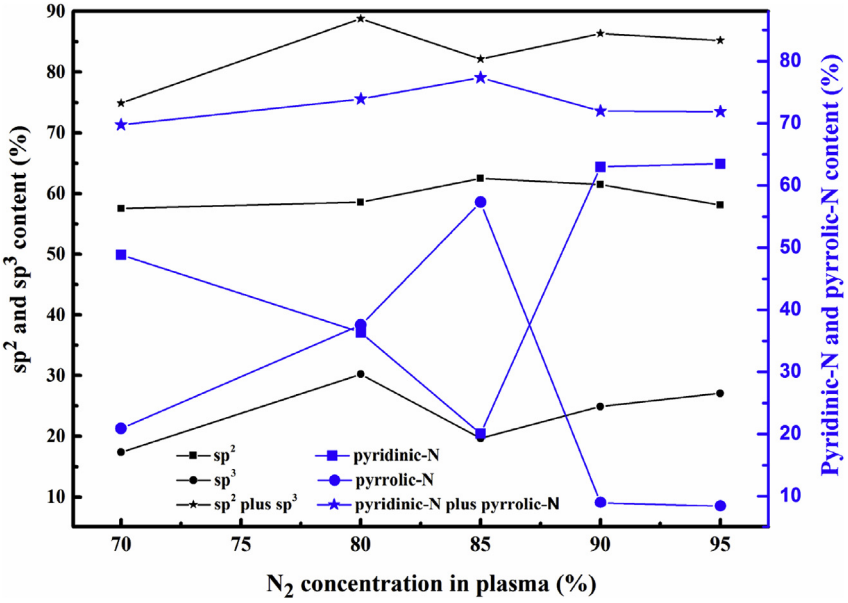

Fig. 7. Values of fitting results of C1s and N1s core-energy level spectra of NCD films with different nitrogen concentrations.

polyacetylene (trans-PA), which are attributed to the C-H wagging monde and/or C-C stretching modes (ν_1) and C=C stretching modes (ν_3) of trans-PA chains.

The fraction and full width at half maximum (FWHM) of different peaks of deposited NCD films are used to analysis the deposited films [38]. The ratio of peak intensity of D-band and G-band to the sum intensity of all peaks was calculated and it is presented as I_D/I_{sum} and I_G/I_{sum} in Fig. 9(a). The FWHM of D-band and G-band are presented in Fig. 9(b). The intensity of two vibration modes of trans-PA, ν_1 and ν_3 mode, to the sum intensity of all peaks are presented in Fig. 9(c) as $I_{\nu1}/I_{sum}$ and $I_{\nu3}/I_{sum}$. Both of the I_D/I_{sum} and I_G/I_{sum} values increase with N_2 concentration in plasma at first, and then decrease with the further increasing of N_2 concentration. This means that the sp^2 content in deposited NCD samples increased first and then decreased when the N_2 concentration kept increasing. The increase of the intensity of D-band is more dramatically than the G-band, which indicates the grain boundary network increase as the grain size decrease when proper concentration of N_2 was inducted into the plasma. The varying tendency of D-band and G-band fraction is consistent with fitness results of XPS C1s core-energy spectra in Fig. 7 as we expected. And the peak position slightly moved to lower wave numbers when the N_2 concentration increase from 70% to 85% and moved back to the higher wave number when the N_2 concentration kept increased to 95%. The FWHM value of D-band and G-band both reach minimum when the nitrogen concentration is 85% as it is shown in Fig. 9(b). Opposite to the changes of D-band and G-band the intensity of trans-PA to the sum of all peaks decreased with the increasing concentration of N_2 first and then increase when the N_2 concentration kept increasing. The decrease of the intensity of peak 1150 cm^{-1} means the decreasing amount of H bonded to trans-PA chains at grain boundaries [35] when the N_2 concentration increase from 70% to 85%. The intensity of peak 1150 cm^{-1} increases when the N_2 concentration kept increasing to 95%. This indicates that the concentration of nitrogen in plasma play an important role in the construction of grain boundaries as deduced before.

It is generally believed that the doped nitrogen atom is more likely to locate in the grain boundaries of NCD films and the structure of doped nitrogen atoms is a crucial factor that can affect

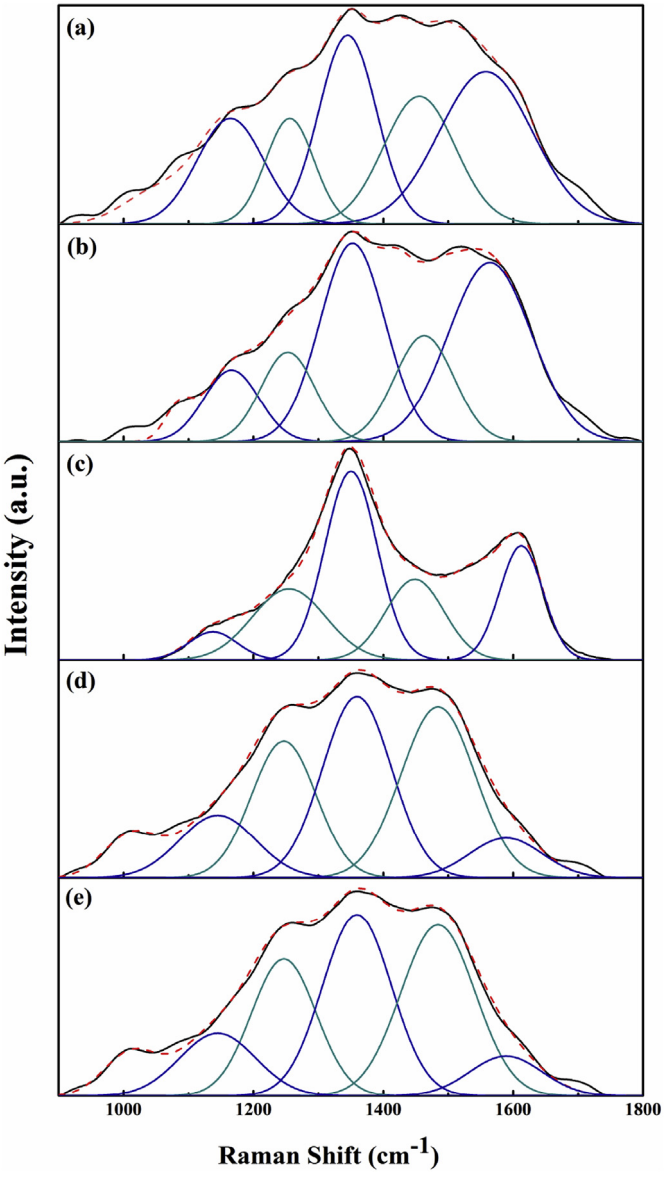

Fig. 8. Visible Raman spectra of NCD films deposited with different nitrogen concentrations: (a)-S1, (b)-S2, (c)-S3, (d)-S4, (e)-S5.

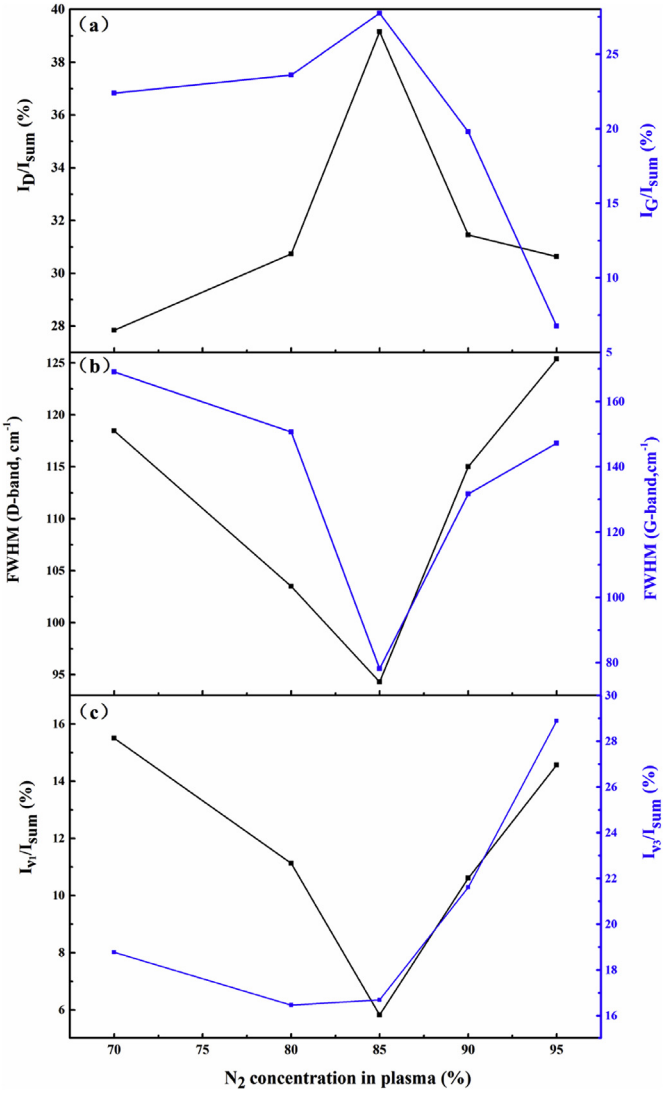

Fig. 9. Values of (a) I_D/I_{sum} and I_G/I_{sum}, (b) FWHM of D-band and G-band of deposited NCD films, (c) $I_{\nu1}/I_{sum}$ and $I_{\nu3}/I_{sum}$.

the surface conductivity [15,25]. As it is shown in Fig. 5, all samples were successfully doped with nitrogen atom and the atom concentration of nitrogen is 1.14%, 1.26%, 1.44%, 1.79% and 2.12% for sample 1 to sample 5, which means that the increasing of nitrogen concentration in plasma is accompanied with the increasing of the nitrogen atom concentration of deposited films. In order to better analysis the construction of doped nitrogen atoms, the XPS N1s core-energy spectra were collected. The N1s spectra with a Shirley type background and Gussian fitting of all samples are presented in Fig. 10. Four peaks are found: (1) peak of pyridinic-N (398.7 ± 0.2 eV, named as N1) [39], (2) peak of amino-N (399.4 ± 0.2 eV, named as N2) [40], (3) peak of pyrrolic-N (400.3 ± 0.2 eV, named as N3) [39], (3) peak of quaternary nitrogen (401.4 ± 0.2 eV, named as N4) [39]. An obvious shift from 399.3 eV to 398.9 eV was found and N1s peak shift to the lower binding energy was caused by a large amount of the existence of amino-N in the deposited films. Compared with N2 the influence of N4 of the spectra is insufficient as the content is much less, and other researchers already had similar results [41]. The decreasing intensity of peak N1 is corresponding of the increasing intensity of peak N3 meanwhile the rising of peak N1 is accompanied with the reducing of peak N3 as it is shown in Fig. 7. The minimum value of peak N1 and the maximum value of peak N3 are obtained when the nitrogen concentration is 85%. The sum of pyridinic-N and pyrrolic-N is almost unchangeable. In the pyridinic-N situation, each nitrogen atom contributes one p-electron to the aromatic π system [42]. For pyrrolic-N, each nitrogen atom contributes two p-electrons [42]. Quaternary nitrogen is also known as “substituted nitrogen” in which nitrogen atoms are incorporated into the deposited films and replace carbon atoms at grain boundaries [42]. Some studies showed that the enhancement of conductivity of deposited films is attributed to the existents of pyridinic-N and/or pyrrolic-N [43]. In our study we found out that compared with the dramatic varying of the surface conductivity the value of pyridinic-N plus pyrrolic-N is fixed.

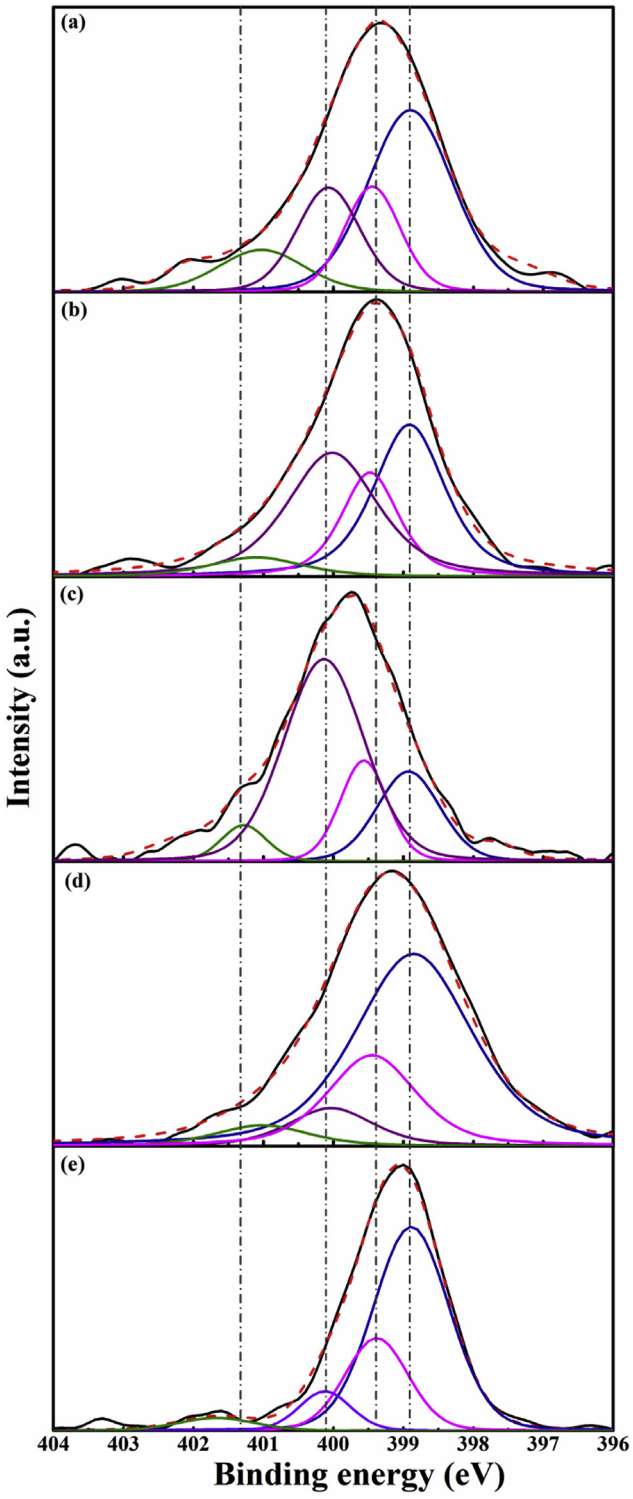

Fig. 10. N1s core-energy level spectra for NCD films deposited with different nitrogen concentrations: (a)-S1, (b)-S2, (c)-S3, (d)-S4, (e)-S5.

4. Conclusion

In this work nitrogen incorporated NCD films are deposited within a nitrogen rich atmosphere by microwave plasma chemical vapor deposition. The N_2 concentration in plasma can obviously affect the growth, surface morphology, grain size, chemical bond of carbon atoms at grain boundaries. Analytical results showed that the surface conductivity is changing with the grain size of NCD films. The lowest resistance was corresponding to the smallest grain size when the nitrogen concentration was 85% in plasma. The fitting results showed that the N_2 concentration was not only varied the content of sp^2 bonded carbon atoms but also affected the structure of sp^2 bonded carbon atoms. The content of the incorporated nitrogen atoms were kept increasing when the N_2 concentration in plasma increased from 70% to 95%, but the concentration of pyridinic-N and pyrrolic-N was almost constant. So we believe that within nitrogen rich atmosphere the N_2 concentration can influence the surface conductivity by incorporated nitrogen atoms and varied the content and the chemical bond of sp^2 carbon atoms in deposited NCD samples.

Acknowledgements

This work was supported by the Natural Science Foundation of China (No. 11175137) and the Project of Hubei Provincial Department of Education (Q20151517).

References

[1] Y. Mokuno, A. Chayahara, H. Yamada, Synthesis of large single crystal diamond plates by high rate homoepitaxial growth using microwave plasma CVD and lift-off process, Diam. Relat. Mater 17 (2008) 415–418.
[2] Dai Huangda, Zhou Kesong, The Preparation Technology and Application of Depositing Diamond Film, M. Metallurgical Industry Press, 2001.
[3] M. Schwander, K.A. Partes, A review of diamond synthesis by CVD processes, J. Diam. Relat. Mater 20 (2011) 1287–1301.
[4] D. Lu, H.D. Li, S.H. Cheng, Fabrication and characteristics of nitrogen-doped nanocrystalline diamond/p-type silicon heterojunction, J. Nano-Micro Lett. 2

(2010) 56–59.
[5] V.V. Siva Kumar, Nnaocrystalline diamond films growth by microwave ECR CVD: studies of structural and photoconduction properties, Vacuum 131 (2016) 259–263.
[6] Andre Guinier, X-ray diffraction, in: Crystals, Imperfect Crystals, and Amorphous Bodies, M. W. H. Freeman and Company, San Francisco, 1963.
[7] Diane S. Knight, William B. White, Characterization of diamond films by Raman spectroscopy, J.J Mater Res. 4 (1989) 385–393.
[8] Orlando, Anirudha V. Sumant, Status review of the science and technology of ultranannocrystalline diamond (UNCD™) films and application to multifunctional deviced, Diam. Relat. Mater 19 (2010) 699–718.
[9] D. Zhou, D.M. Gruen, L.C. Qin, Control of diamond film microstructure by Ar additions to CH_4/H_2 microwave plasmas, J. Appl. Phys. 84 (1998) 1981–1989.
[10] E.M.A. Fuentes-Fernadez, J.J. Alcantar-Pena, G. Lee, et al., Synthesis and characterization of microcrystalline diamond to untrananocrystalline diamond films via hot filament chemical vapor deposition for scalling to large area applicaition[J], Thin Solid Films 603 (2016) 62–68.
[11] J. Birrell, J.A. Carlise, O. Auciello, et al., Morphology and electronic structure in nitrogen-doped unltrananocrytalline diamond, Appl. Phys. Lett. 81 (2002) 2235–2237.
[12] T.D. Corrigan, D.M. Gruen, A.R. Krauss, The effect of nitrogen addition to Ar/CH_4 plasmas on the growth, morphology and field emission of ultrananocrystalline diamond, Diam. Relat. Mater 11 (2002) 43–48.
[13] Q. Chen, D.M. Gruen, A.R. Krauss, The structure and electrochemical behavior of nitrogen-containing nanocrystalline diamond films deposited from CH_4/N_2/Ar mixtures, J. Electrochem Soc. 148 (2001) 1551–1560.
[14] K.L. Ma, W.J. Zhang, Y.S. Zou, Electrical properties of nitrogen incorporated nanocrystalline diamond films, Diam. Relat. Mater 15 (2006) 626–630.
[15] Kalpataru Panda, Huang-Chin Chen, B. Sundaravel, et al., Direct observation of enhanced emission sites in nitrogen implanted hybrid structured ultrananocrystalline diamond films, J. Appl. Phys. 113 (2013) 1–8.
[16] Kalpataru Panda, B. Sundaravel, B.K. Panigrahi, et al., Structural and electronic properties of nitrogen ion implanted ultra nanocrystalline diamond surfaces, J. Appl. Phys. 110 (2011) 1–9.
[17] A.V. Sumant, A.R. Krauss, D.M. Gruen, et al., Ultrananocystalline diamond film as a wear- resistant and protective coating for mechanical seal applications, Tribol. Trans. 48 (2005) 24–31.
[18] A.R. Konicek, D.S. Grierson, P.U. Gilbert, et al., Origin of ultralow fricition and wear in ultrananocrystalline diamond, Phys. Rev. Lett. 100 (23) (2008) 235502.
[19] O. Auciello, A.V. Sumant, C. Goldsmith, et al., Fundamentals and technology for monolithically integrated RF-MEMS switches with ultrananocrystalline diamond dielectric/CMOS devices, micro-and nanotechnology sensors, systems, and applications-II, Proc. SPIE 7679 (2010) 76791K1.
[20] V.P. Adiga, A.V. Sumant, S. Suresh, et al., Mechanical stiffness and dissipation in ultrananocrystalline diamond micro-resonators, Phys. Rev. B 79 (2009) 245403.
[21] O.A. Williams, Ultrananocrystalline diamond for electronic applications, J.Semicond Sci. Tech. 21 (2006) 49–56.
[22] K.L. Ma, W.J. Zhang, Y.S. Zou, Y.M. Chong, et al., Electrical properties of nitrogen incorporated nanocrystalline diamond films, Diam. Relat. Mater 15 (2006) 626–630.
[23] Y.K. Liu, P.L. Tso, D. Pradhan, I.N. Lin, M. Clark, Y. Tzeng, Structural and electrical properties of nanocrystalline diamond (NCD) hravily doped by nitrogen, Diam. Relat. Mater 14 (2005) 2059–2063.
[24] X.J. Hu, J.S. Ye, H.J. Liu, Y.G. Shen, et al., n-type conductivity and phase transition in ultrananocrystalline diamond by oxygen ion implantation and annealing, J. Appl. Phys. 109 (2011) 1–7.
[25] J. Birrell, J.E. Gerbi, O. Auciello, Bonding structure in nitrogen doped ultrananocrystalline diamond, J. Appl. Phys. 93 (2003) 5606–5612.
[26] Philipp R. Heck, Frank J. Stadermann, Dieter Isheim, et al., Atom-probe analyses of nanodiamonds from Allende, Meteorit. Planet. Sci. 49 (2014) 453–467. Nr3.
[27] O.A. Williamsa, M. Daenen, J.D.' Haen, Comparison of the growth and properties of ultrananocrystalline diamond films deposited from CH_4/N_2/Ar mixtures, J. Electronchem Soc. 148 (2001) 1551–1560.
[28] S.T. Chen, Y.C. Chu, C.Y. Liu, Surface-enhanced Raman spectroscopy for characterization of nanodiamond seeded substrates and ultrananocrystalline diamond at the early-stage of plasma CVD growth process, Diam. Relat. Mater 24 (2012) 161–166.
[29] Huang-Chin Chen, Chuan-Sheng Wang, I-Nan Lin, Hsiu-Fung Cheng, Defect structure for the ultra-nanocrystalline diamond films synthesized in H_2-containing Ar/CH_4 plasma, Diam. Relat. mater 20 (2011) 368–373.
[30] E.M.A. Fuentes-Fernandez, J.J. Alcantar-Pena, G. Lee, et al., Synthesis and characterization of microcrystalline diamond to ultrananocrystalline diamond films via hot filament chemical vapor deposition for scaling to large area applicaitions, Thin Solid Films 603 (2016) 62–68.
[31] Chii-Ruey Lin, Wen-Hsiang Liao, Da-Hua Wei, et al., Formation of ultrananocrystalline diamond films with nitrogen addition, Diam. Relat. mater 20 (2011) 380–384.
[32] K.L. Ma, W.J. Zhang, Y.S. Zou, Electrical properties of nitrogen incorpotated nanocrystalline diamond films, Diam. Relat. Mater 15 (2006) 626–630.
[33] S. Al-Riyami, S. Ohmagari, T. Yoshitake, X-ray photoemission spectroscopy of nitrogen-doped UNCD/a-C: H films prepared by pulsed laser deposition, J. Diam Relat Mater. 19 (2010) 510–513.
[34] M. Rybin, A. Pereaslavtsev, T. Vasilieva, et al., Efficient nitrogen doping of graphene by plasma treatment, Carbon 96 (2016) 196–202.
[35] Xiaojun Hu, Chengke Chen, Shaohua Lu, High mobility n-type conductive unltrananocrystalline diamond and grapheme nanoribbon hybridized carbon films, Carbon 98 (2016) 671–680.
[36] Sausan Al-Riyami, Shinya Ohmagari, Tsuyoshi Yoshitake, X-ray photoemission spectroscopy of nitrogrn-doprd UNCD/a-C: H films prepared by pulsed laser deposition, Diam. Ralate Mater 19 (2010) 510–513.
[37] Y.L. Li, X.X. Xia, Effect of grain boundary on local surface conductivity of diamond film, J. Appl. Phys. 105 (2009).
[38] O.A. Williams, M. Nesládek, Growth and properties of nanocrystalline diamond films, J. Phys. Status Solidi Appl. Mater. 203 (2006) 3375–3386.
[39] W.J. Gammon, O. Krafe, A.C. Reilly, B.C. Holloway, Experimental comparison of N(1s) X-ray photoelectron spectroscopy binding energies of hard and elastic amorphous carbon nitride films with reference organic compounds, Carbon 43 (2003) 1917–1923.
[40] J.R. Pels, F. Kaptejin, J.A. Moulijin, Q. Zhu, et al., Evolution of nitrogen functionalities in carbonaceous materials during pyrolysis, Carbon 33 (1995) 1641–1653.
[41] L.C. Qin, D. Zhou, A.R. Krauss, D.M. Gruen, Tem characterization of nanodiamond thin films, Nanostructured Mater. 10 (1998) 649–660.
[42] J.R. Pels, F. Kapteijn, J.A. Moulijin, Evolution of nitrogen functionalities in carbonaceous materials during pyrolysis, Carbon 33 (1995) 1641–1653.
[43] Y. Shao, Nitrogen-doped graphene and its electrochemical applications, J. Mater Chem. 20 (2010) 7491–7496.